Carbohydrate Polymers 88 (2012) 481–489

Contents lists available at SciVerse ScienceDirect

Carbohydrate Polymers

journal homepage: www.elsevier.com/locate/carbpol

The rheological behavior of native and high-pressure homogenized waxy maize starch pastes

Bao Wang[a,1], Li-jun Wang[b,1], Dong Li[a,*], Qing Wei[a], Benu Adhikari[c]

[a] College of Engineering, China Agricultural University, P. O. Box 50, 17 Qinghua Donglu, Beijing 100083, China
[b] College of Food Science and Nutritional Engineering, China Agricultural University, Beijing, China
[c] School of Health Sciences, University of Ballarat, VIC 3353, Australia

ARTICLE INFO

Article history:
Received 30 October 2011
Received in revised form
11 December 2011
Accepted 15 December 2011
Available online 23 December 2011

Keywords:
Rheological properties
Waxy maize starch
Gelatinization
High-pressure homogenization
Thickening

ABSTRACT

Both steady and large amplitude dynamic rheological testes were carried out in hydrothermally gelatinized waxy maize starch (WMS) pastes. The concentration of WMS was maintained at 6.0% (w/w) throughout these tests. The WMS pastes exhibited shear thickening behavior during the first up curve in steady shear tests. The shear thickening behavior was found to be irreversible and could not be retained after equilibrating the pastes beyond 6 h. The change in the shape of Lissajous curves was insignificant during strain sweeps at higher angular frequencies. This arose because of slow response of WMS pastes to oscillatory strain within a period of oscillatory shear, which can be attributed to the domination of rheological properties by amylopectin in continuous phase. High-pressure homogenization (HPH) was found to significantly reduce the apparent viscosity of the WMS pastes. After HPH, the WMS pastes behaved like typical Newtonian fluids.

1. Introduction

Starch is a main component of foods and it is also commonly used as an ingredient for thickening and gelling. Since the rheological behavior of starch paste and suspensions is very important in processing, the rheological properties of starch pastes or suspensions are quite intensively investigated. Unlike normal starch (amylose content between 20 and 30%, w/w) and high-amylose starch (amylose content >50%, w/w), waxy starch contains only traces of amylose (Achayuthakan & Suphantharika, 2008; Preiss, 1991). Due to the unique composition (i.e. 100% amylopectin), waxy starch is reported to be a promising raw material in food, medicine, and cosmetic industries (Lehmann, Volkert, Fischer, Schrader, & Nerenz, 2008; Sands, Leidy, Hamaker, Maguire, & Campbell, 2009). The knowledge of rheological behavior of the food ingredients (such as starch pastes) is important to optimize applicability, stability and sensory properties of end products (Kulicke, Eidam, Kath, Kix, & Kull, 1996). Waxy starch paste is an ideal biphasic model for rheological study. This is because the pastes of waxy starch contain both degraded starch granules and a continuous matrix of amylopectin, which makes such suspensions ideal model for the investigation of rheological properties of biphasic model fluids (Rodríguez-Hernández, Durand, Garnier, Tecante, & Doublier, 2006). In these systems, due to the absence of amylose, the complexity of the paste system can be simplified. In addition, to waxy starch pastes the effects of gelation and retrogradation on the rheological properties caused by amylose can also be avoided.

Because of the purity of amylopectin, the paste obtained from waxy starch is reported to have quite different rheological properties from those obtained from common starch and high-amylose starch. For examples, waxy starch pastes have different thixotropic properties from the pastes obtained from the corresponding common and high-amylose starches. The anti-thixotropic property which features a counter-clockwise loop of shear stress/apparent viscosity versus shear rate during the steady shear cycle (involving a rate ramp up to a peak shear rate, then a ramp down back to zero) is mostly reported for waxy starches (Wang, Li, Wang, & Özkan, 2010). Furthermore, shear thickening property is essentially reported for waxy starch during the shear tests, indicating the existence of quite different flow properties in waxy starch compared to other starches (Wang, Wang, Dong Li Zhou, & Özkan, 2011).

The investigation of the shear-thickening behavior of waxy maize starch (WMS) pastes with relatively low concentrations (<10%, w/w) was initiated by Dintzis et al. (Dintzis & Bagley, 1995; Dintzis, Berhow, Bagley, Wu, & Felker, 1996). Dintzis and Bagley (1995) showed that the waxy starch suspensions (3%, w/w) gelatinized using 0.2 M sodium hydroxide (without starch particle

* Corresponding author. Tel.: +86 10 62737351; fax: +86 10 62737351.
E-mail address: dongli@cau.edu.cn (D. Li).
[1] These authors contributed equally to this work.

0144-8617/$ – see front matter © 2011 Elsevier Ltd. All rights reserved.
doi:10.1016/j.carbpol.2011.12.028

Nomenclature

K	consistency index, Pa s^n
n	flow behavior index, dimensionless
R^2	correlation coefficient, dimensionless
$\dot{\gamma}$	shear rate, s^{-1}
γ	shear strain, dimensionless
γ_o	maximum shear strain within a period of oscillatory shear, dimensionless
η^*	complex viscosity, Pa s
η_a	apparent viscosity, Pa s
τ	shear stress/oscillatory stress, Pa
τ_0	maximum oscillatory stress within a period of oscillatory shear, Pa
ω_o	constant angular frequency in strain sweep, rad/s

ghosts) can display shear-thickening behavior. When the amylose and amylopectin fractions were separated from normal potato starch and the rheological behavior of each fractions were investigated, it was found that only the dispersed amylopectin fraction displayed shear thickening behavior (Dintzis et al., 1996). As a result, shear thickening was ascribed to free amylopectins by Dintzis et al. (1996). In subsequent study, Kim, Willett, Carriere, & Felker (2002) reported similar shear thickening behavior in starch pastes obtained using gentle alkali-gelatinization, and ascribed shear thickening in these pastes to the breaking up of the highly concentrated gel-like starch clusters during the tests, which caused increase in effective starch concentration. Wang et al. (2011) gelatinized the waxy maize starch using hydrothermal method coupled with strong agitation and found that the pastes obtained in this way also displayed shear-thickening behavior. They also found that the shear thickening behavior was related to both temperature during the tests and starch concentration used.

In many physiological processes such as mastication and swallowing, the deformation is large and rapid. This necessitates that the non-linear viscoelastic characteristics be measured and quantified. Large amplitude oscillatory shear (LAOS), which is normally generated by a strain sweep test, can produce a measurable nonlinear material response in the fluids (Hyun, Kim, Ahn, & Lee, 2002; Hyun et al., 2011). LAOS behavior of the fluids was reported to be associated with formulation details (material composition and microstructure), and is very sensitive to the interactions or the shear-induced formation of microstructures of complex fluids (Hyun et al., 2002; Leblanc, 2007). The LAOS behavior of the WMS pastes was also studied in this study.

After gelatinization, mechanical treatments during downstream processing such as mixing, extrusion, pumping and homogenization directly affect the rheological properties of starch pastes or suspensions. It is reported that shear rates of 1 to 10^2 s^{-1} in extrusion, 1 to 10^3 s^{-1} in tube flow mixing and pumping and up to 10^5 s^{-1} in high-pressure homogenization (HPH) are very common in food industry (Barnes, Hutton, & Walters, 1989; Loh, 1992; Nayouf, Loisel, & Doublier, 2003). Due to very high energy input per mass of a product, HPH can usually introduce new and surprising changes in products. To our knowledge, only limited studies are so far carried out in order to study the effect of HPH on rheological properties of polysaccharide solutions. Viturawong, Achayuthakan, and Suphantharika (2008) prepared xanthan gum solutions of different molecular weights by using HPH at 70 MPa with different numbers of passes. This study showed that the addition of xanthan gum with a higher molecular weight had a more pronounced effect on rheological properties of rice starch pastes. Che et al. (2009) applied HPH up to 100 MPa in 2.0% (w/w) potato and cassava starch slurries, and reported significant decrease in apparent viscosity. However, the effect of HPH on rheological properties of waxy starches or special starches which have no amylose is still unavailable.

The objectives of this study were to investigate the effects of preshearing and conditioning time, testing mode (steady shear/large amplitude oscillatory shear), as well as homogenization pressure on rheological properties of the waxy maize starch pastes. We believe this study provides comprehensive understandings and new insights into rheological properties of WMS pastes which can be applied to various production processes in food processing industries.

2. Materials and methods

2.1. Materials

Commercial waxy maize starch (amylose content < 1%, w/w) was purchased from Jinan Jinwang Food Co., Ltd. (Shandong Province, China). The moisture content of the starch was determined by drying sample in an air-oven maintained at 105 °C to constant weight. Triplicate drying experiments were carried out and the average value of those experiments was 9.71% (w/w). Commercial normal maize starch (22% amylose, w/w) was purchased from Weizhiyuan Food Co., Ltd. (Beijing, China), and the moisture content was determined to be 11.35% (w/w).

2.2. Preparation of waxy maize starch (WMS) suspensions

The WMS slurries with WMS concentration of 6.0% (w/w) were prepared by dispersing calculated amount of WMS (dry basis) into distilled water to make a total weight of 150 g. Subsequently, the well mixed WMS slurry (150 g) was transferred to a conical flask (250 ml), and heated in a water bath at 95 °C for 40 min. The mixing rate was 450 rpm during gelatinization. The mixing/agitation rate during the gelatinization process was controlled by a digital mixer (EUROSTAR, IKA Instruments, Germany). Once the pasting/gelatinization process was completed, the samples were rapidly cooled in another water bath. For reference, the 6.0% (w/w) normal maize starch (NMS) pastes were prepared in the same way. The cooled samples were equilibrated in an incubator at 25 °C for 2 h before measurement. For replicate tests, fresh samples were prepared to ensure the consistency and accuracy.

2.3. Steady shear test of WMS pastes

Steady flow properties of the samples were determined using an AR2000ex rheometer (TA Instruments Ltd, Crawley, UK) at 25 °C. An aluminum parallel plate geometry (40 mm diameter) was used and the gap size was set as 1.0 mm during all the tests. Before testing, a thin layer of silicone oil was applied on the edge of the sample in order to prevent moisture evaporation. Continuous-ramp steady shear measurements of the WMS pastes (6.0%, w/w) were performed at 25 °C to obtain shear stress/apparent viscosity versus shear rate data.

Both the logarithmic mode and linear mode of shear rate ramp were adopted. For the tests conducted in log mode, the stepped-ramp shear rate was programmed to logarithmically increase from 0.1 to 500.0 s^{-1} followed immediately by a logarithmical reduction in the shear rate from 500.0 to 0.1 s^{-1}. Fourteen points were collected per decade for both the ramping-up and ramping-down steps. In the case of linear mode, the shear rate was programmed to linearly increase from 1.0 to 500.0 s^{-1} within 6 min. It was followed immediately by a linear decrease from 500.0 to 1.0 s^{-1} at the same time scale. For comparison, continuous-ramp steady shear measurements of the NMS pastes (6.0%, w/w) were performed at 25 °C in linear mode.

The power law model (Eq. (1)) was fitted to the experimental data both from the ascending and descending segments of the shear cycle:

$$\tau = K\dot{\gamma}^n \quad (1)$$

where τ is the shear stress (Pa), $\dot{\gamma}$ is the shear rate (s^{-1}), K is the consistency index (Pa s^n), and n is the flow behavior index (dimensionless).

2.4. Dynamic strain sweep

The effects of strain loop as well as pre-shearing on the dynamic rheological properties of the WMS pastes were tested in this section. The dynamic strain sweeps of the 6.0% (w/w) WMS suspensions were performed at 25 °C. The strain was increased from 1.0% to 2000.0% linearly at ω_0 of 30 rad/s. This step was followed immediately by a linear reduction of the strain from 2000.0% to 1.0%. This was followed once again by the linear increase in the strain from 1.0% to 2000.0%. Besides, the 6.0% (w/w) WMS suspension was pre-sheared at 600 s^{-1} for 1 min. The same strain sweep procedure was subsequently performed to examine the effect of pre-shearing on the dynamic rheological properties of the WMS pastes. In each experiential runs, a thin layer of silicone oil was applied on the edge of the sample in order to prevent evaporation.

2.5. High-pressure homogenization on rheological properties of WMS pastes

The 6.0% (w/w) WMS pastes were homogenized using a high-pressure homogenizer (AH100D, ATS Engineering Inc, Italy) at different homogenizing pressures (25, 50, 75, 100, and 125 MPa). Two hundred ml sample was processed in a batch throughout these tests. The WMS pastes without HPH treatment was used as a reference. After high-pressure homogenization, the samples were equilibrated at normal atmospheric pressure in an incubator at 25 °C for 1 h before further measurements. Continuous steady shear tests in a linear mode (as described in Section 2.3) were carried out at 25 °C to obtain shear stress/apparent viscosity versus shear rate data.

2.6. Microscopy study of starch pastes

To investigate the microstructure of the starch pastes, samples in this study were observed using an optical microscope (CX31 Biological Microscope, Olympus Corporation, Japan) equipped with an CCD camera module. Micrographs were recorded at magnification of 100×, and a bar has been added on each picture to indicate the real size of the microstructure.

2.7. Statistical analysis

All experiments described above were carried out in triplicates for each sample. The data presented were the means and standard deviations of each experiment. A one-way analysis of variance (ANOVA) and Tukey's test were used to establish the significance of differences among the mean values at 0.95 confidence level. The statistical analyses were performed using SPSS (2003) version 13.0 for Windows program (SPSS Inc., Chicago, USA).

3. Results and discussion

3.1. Steady flow properties of WMS pastes

A typical microphotograph of 6% (w/w) WMS paste showing its gel microstructure after gelatinization by hydrothermal method (described in Section 2.2) is given in Fig. 1(A). From Fig. 1(A), it can be observed that most of the WMS granules were dissolved into the continuous phase during the gelatinization process. The microphotograph also shows that some starch ghost particles and degraded fragments still exist in the gelatinized paste. It is generally accepted that when starch is heated in excess water, starch granules swell and increase in volume. During this gelatinization process some of the starch components such as amylopectin dissolve into the continuous phase, leading to a suspension of swollen particles embedded in the macromolecular continuous phase (Mendez-Montealvo, Wang, & Campbell, 2011). Unlike natural granules of starch, starch ghost particles in gelatinized WMS are reported to have much lower robustness and are formed due to cross-linking of the polysaccharide chains within swollen granules (Debet & Gidley, 2007). For comparison, microscopic structure of the 6% (w/w) normal maize starch (NMS) paste (produced by the same gelatinization method) is also provided (Fig. 1(B)). It can be observed from Fig. 1 that the microscopic structure of WMS paste is distinctly different from that of the NMS. Due to the absence of amylose in the continuous phase, the WMS paste had better clarity than the corresponding NMS paste. Because of the presence of amylose in the continuous phase, the microstructure of NMS paste became much more complicated. Amylose is capable of forming crosslinking network structure in the continuous phase quite rapidly during cooling. This behavior of amylose leads to gelation and retrogradation of the amylose containing starch paste. It is reported that amylose fraction of gelatinized starch can complete the retrogradation process within few hours (Kaur, Singh, Singh, & McCarthy, 2008).

Fig. 2(A) gives the apparent viscosity (η_a) versus shear rate (s^{-1}) curves of both WMS and NMS pastes measured during continuous shear rate mode. From Fig. 2(A), it can be seen that the 6% (w/w) WMS paste displays both shear thinning and shear thickening (within the shear rate range of 40–100 s^{-1}) behaviors in the up curve. Because of the difference in composition and paste structure, pastes from WMS and NMS have different rheological properties. Furthermore, the 6% (w/w) WMS paste also displays a counter-clockwise hysteresis loop from the up and down curves, indicating an anti-thixotropic behavior. Unlike WMS paste, the 6% (w/w) NMS paste shows common shear-thinning and thixotropic properties (i.e. clockwise hysteresis loop) as shown in Fig. 2(A). These data indicate that the WMS paste has distinctly different steady rheological properties compared to that of NMS paste. It has to be noted that shear thickening is time-independent increase in the apparent viscosity as a function of increasing shear rate (Indei, 2007; Steffe, 1996), while anti-thixotropy reflects the time-dependent thickening of the solutions (Gouveia, Muller, Marchal, & Choplin, 2008; Steffe, 1996). It is known that solutions/suspensions with anti-thixotropic behavior either display counter-clockwise hysteresis loop during shear cycles or display increasing apparent viscosities under constant shear rate.

Dintzis et al. (1996) suggested that the shear-thickening behavior of waxy starch pastes can be attributed to the presence of amylopectin in the continuous phase. As the shear rate increases during the first up curve, the free amylopectin in the continuous phase forms a more stable microscopic network-structure which leads to the increase in the viscosity of the paste (Dintzis et al., 1996). In this study, the WMS pastes displayed similar flow curves with almost the same shear-thickening behavior from both logarithmic and linear shear tests as indicated in Fig. 2(A) and (B). However, such shear-thickening behavior was not observed in the down curves, indicating the shear irreversibility in such a property. As shown in Fig. 2(B) (log mode of shear rate), three shear cycles were performed for the 6% (w/w) WMS pastes, and only the first up curve displayed shear thickening. After the first up curve, the flow curves only displayed

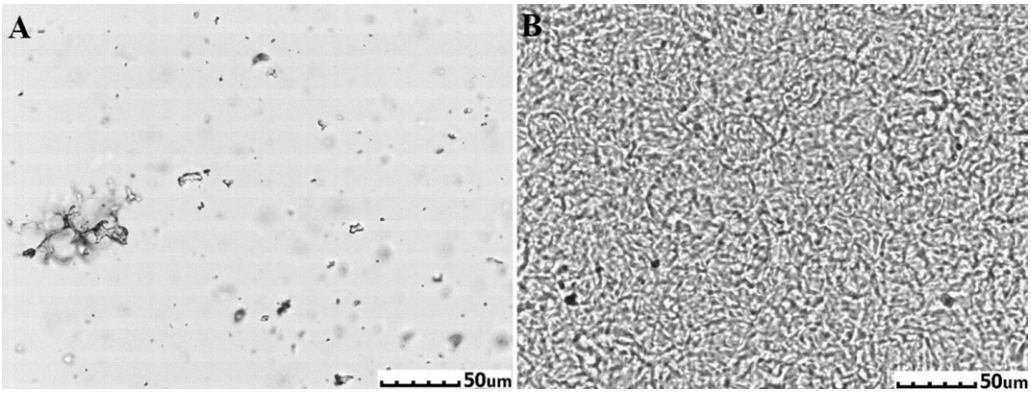

Fig. 1. Typical microphotographs of the 6.0% (w/w) pastes from both waxy maize starch and normal maize starch gelatinized by hydro-thermal method (95 °C, 40 min and 450 rpm): (A) paste from waxy maize starch, (B) paste from normal maize starch.

shear-thinning behavior, and superimposed in a good manner, indicating a stable pseudoplastic behavior. As discussed previously (Section 1), Kim et al. (2002) attributed the shear-thickening behavior to the breaking down of the concentrated clusters of gelatinized starch granules, which causes an increase in the effective starch concentration. This theory adequately explains the irreversibility in the shear-thickening behavior observed in our experiments. However, it is unable to explain the different rheological behaviors observed between pastes from normal starch and waxy starch gelatinized at identical conditions (as shown in Fig. 2(A)).

In order to study the shear rate dependence of shear-thickening, few shear rates (5, 20, 72, and 192 s^{-1}) within, slightly below and above the shear-thickening region were held for up to 3 min and the corresponding flow curves were measured (Fig. 2(C)–(F)). It can be observed that the shear thickening occurs within the shear rate range of 40–100 s^{-1}. From Fig. 2(C) and (F) that it can also be seen that when shear rate was held at 5 and 192 s^{-1}, the resultant flow curves showed no change in curves of apparent viscosity. When shear rate was held at 20 s^{-1} for 3 min, though outside the shear-thickening range, the apparent viscosity displayed a limited increase (Fig. 2(D)). Such a result indicates that the anti-thixotropic behavior can occur at lower shear rates than the anticipated shear rate range at which shear-thickening occurs in 6% (w/w) WMS pastes. However, the shear-thickening curve in Fig. 2(D) still had a similar shape to the one in Fig. 2(B) (first cycle), indicating that the shear rate of 20 s^{-1} is not high enough to induce structural change required for shear-thickening to occur. When shear rate was held at 72 s^{-1} (within the shear-thickening range) for 3 min (Fig. 2(E)), the apparent viscosity increased 15.4% compared to minimum apparent viscosity of 0.70 Pa s at 72 s^{-1}. At the same time, the shape of flow curve has changed remarkably, suggesting such a shear rate

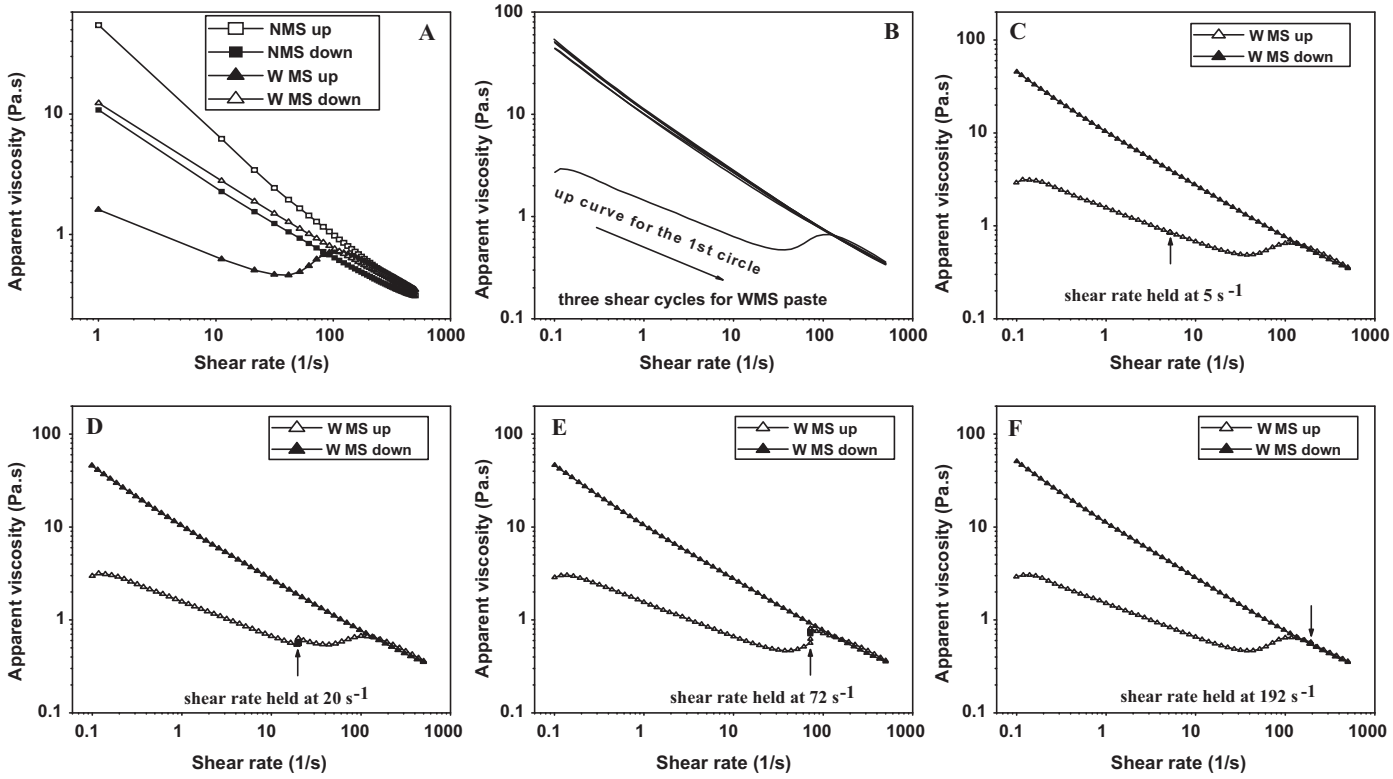

Fig. 2. Flow properties of the 6.0% (w/w) starch pastes tested at different conditions. Steady shear tests in (A) were conducted in a linear mode, while in (B), (C), (D), (E), and (F) were conducted in a logarithmic mode.

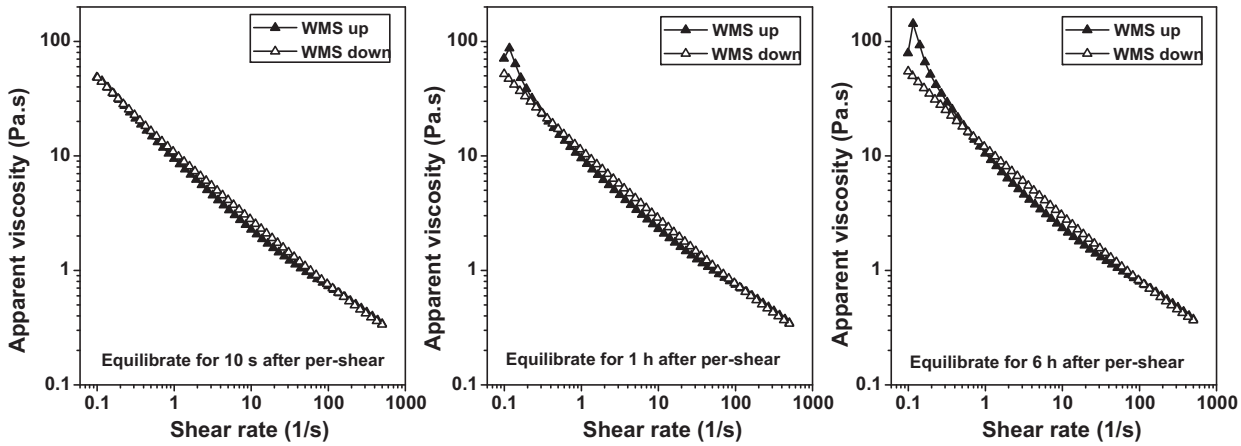

Fig. 3. The effect of equilibration time on the rheological properties of 6.0% (w/w) waxy maize starch pastes after pre-shearing at 600 s^{-1} for 1 min: (A) 10 s after pre-shearing, (B) 1 h after pre-shearing, and (C) 6 h after pre-shearing.

level is high enough to significantly alter the microscopic structure of the continuous phase.

The effect of equilibration after pre-shearing on rheological behaviors of WMS pastes were also studied in this study. The 6% (w/w) WMS pastes were pre-sheared at 600 s^{-1} for 1 min, and subsequently equilibrated within the rheometer at 25 °C for different time sets (10 s, 1 h, and 6 h). After the equilibration step, steady shear tests were performed on the pastes. The flow curves of the WMS pastes with different equilibrating time are given in Fig. 3(A)–(C). After pre-shearing at 600 s^{-1} for 1 min, all WMS pastes with different equilibration time displayed similar flow curves, and only shear thinning behavior was observed. This indicated that no significant ($p < 0.05$) structural recovery occurred during the equilibration process. These results also suggest that structural change responsible for shear-thickening cannot be recovered by equilibrating the samples. Although there still is some degree of difference between the flow curves, for example, between samples equilibrated for 1 h and 6 h, the increase in the apparent viscosity is only marginal (data not shown). Besides, the counter-clockwise hysteresis (indicating anti-thixotropic behavior) in the central part and clockwise hysteresis in left part of the flow loop (indicating thixotropic behavior) became more distinct with increase in the equilibration time. This indicates that both anti-thixotropic and thixotropic properties of WMS pastes can be affected by equilibration.

From the results presented above, it becomes quite clear that the shear-thickening of WMS pastes is very unstable. Though such a shear thickening can be exactly duplicated by parallel tests, this behavior is irreversible and also can be eliminated by pre-shearing the paste at high shear rate. The shear-thickening behavior cannot be retained after equilibrating the paste beyond 6 h. In this study, the WMS paste immediately after hydrothermal pasting (gelatinization) can exhibit shear-thickening at ambient temperature. Therefore, it can be assumed that the paste structure capable to exhibit such a shear-thickening behavior is induced by the pasting or the gelatinization process. As reported previously (Wang et al., 2011), the critical shear rate value required for shear thickening of WMS pastes increases with increasing the testing temperature. With testing temperature of 85 °C, the 6% (w/w) WMS pastes (obtained using the same gelatinization procedure) had a critical onset shear rate of 89.26 ± 5.88 s^{-1} for shear thickening (compared to 41.73 ± 0.01 for tests at 25 °C) (Wang et al., 2011). It is expected that when the pasting (gelatinization) temperature of 95 °C is used, the critical shear rate for onset of the shear-thickening should be even higher. Although we applied the rotational speed of 450 rpm during the gelatinization procedure, the shear rate at this rotational speed would be lower than the critical values and cannot produce shear thickening. After gelatinization, when the WMS pastes were tested with increasing shear rate at 25 °C, the samples with specific microscopic structures were capable of producing shear-thickening at relatively lower shear rates (about 40–100 s^{-1} in this study).

3.2. Dynamic strain sweep tests of the samples

Fig. 4 shows the variation in complex viscosity of WMS pastes as a function of percentage of strain. As shown in Fig. 4(A), in the case of WMS pastes without pre-shearing, strain thickening is observed during the first up curve within strain ranging from 750% to 1300%. Strain thickening can be described as an increase in the complex viscosity (η^*) at critical combinations of strain-amplitude and angular frequency. It is reported that the strain thickening or strain hardening is associated with the strain-stiffening network components, or shear-induced network formation (Hyun et al., 2011). When a critical strain is imposed, the complex microstructure resists the deformation and causes increase in η^*. Above the range of critical strain, the complex microstructure is destroyed by increasing deformation, and the polymer chains thus align with the flow field, which results into decrease in the complex viscosity (Hyun et al., 2002).

This theory explains our experimental observations reasonably well. Once the complex network microstructure is destroyed, the WMS pasts cannot display strain-thickening anymore during subsequent strain sweep cycles. This indicates that no major microstructure change takes place above critical strain value. Similarly, after pre-shearing at 600 s^{-1} for 1 min, the WMS pastes displayed only strain-thinning behavior during all the sweep cycles. This indicates that the network formation responsible for strain-thickening is destroyed completely during the pre-shearing process. A comparison of Fig. 4 panel (A) and (B) shows that the complex viscosity of the WMS pastes increased significantly ($p < 0.05$) after pre-shearing (see 1st up curve), indicating the formation of a more stable microstructure. Furthermore, the η^* versus. γ curves after pre-shearing show distinct clock-wise hysteresis between the 1st (up) and 2nd (down) sweeps, which is suggestive of a thixotropic behavior of the pastes and should be ascribed to the effect of pre-shearing. This is to some degree different from the steady shear tests, in which the 1st and 2nd curves superimposed well after pre-shearing at 600 s^{-1}, and such a difference should be ascribed to the differences between test modes (steady/dynamic shear). However, after the first up sweep, the following sweeps produced similar η^* versus γ curves with good superposition from WMS pastes with or without pre-shearing.

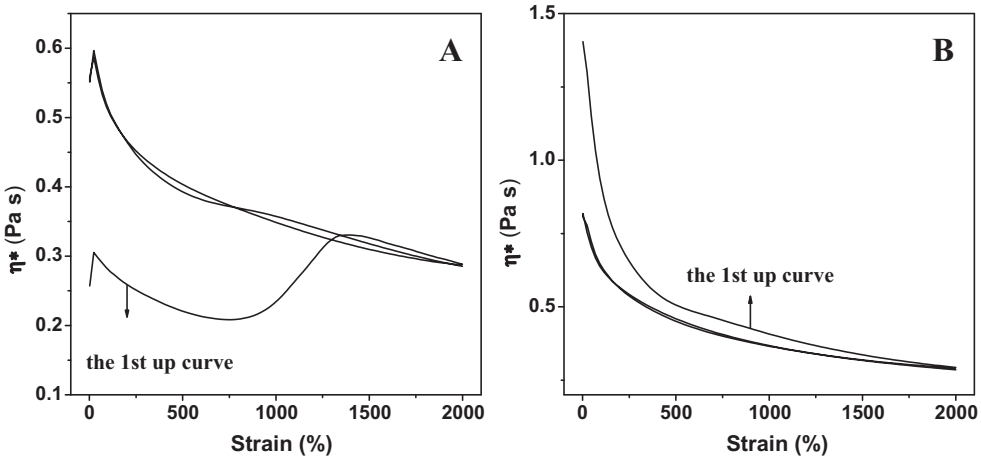

Fig. 4. The effect of pre-shearing on complex viscosity of 6.0% (w/w) waxy maize starch pastes from strain sweep (ω_o = 30 rad/s): (A) without pre-shearing, and (B) with pre-shearing at 600 s^{-1} for 1 min.

3.3. Lissajous plots

In order to better represent the behavior of WMS pastes during strain sweep, the normalized Lissajous curves ($\tau(t)/\tau_o$ versus $\gamma(t)/\gamma_o$ within a period of oscillatory shear during strain sweeps) are given in Fig. 5(A). The Lissajous curves better represent the nonlinear response of the WMS pastes during dynamic deformation. The corresponding strain sweep curves are also provided in Fig. 5(B) for comparison purpose. Wall slip has been postulated to influence the results at high frequency for strain sweeps. And if slip had occurred during the tests, the critical strain required for strain thickening would exhibit a plateau value for high frequencies (Lee & Wagner, 2003). It should be noted here that such a plateau is not observed (see Fig. 5(B)) in this study, and the accuracy of the data can be ensured.

It can be observed in Fig. 5(A) that at lower ω_o of 1 and 10 rad/s, the distortion of the Lissajous curves is significant ($p < 0.05$) with the increase in strain. However, at higher ω_o (70, 100 rad/s) and increase of strain in nonlinear range, the distortion of the Lissajous curves is relatively small, indicating significant effect of angular frequency on dynamic stress response of WMS pastes. Besides, within the strain-thickening range (Fig. 5(B)) of the strain sweeps with a fixed frequency, essentially no distortion in shape of Lissajous curves is observed. It has to be noted here that for the Lissajous curves within the strain-thickening range of strain sweeps (the thickening range is shown in Fig. 5(B)), generally the graphs show an elliptical shape. Such an elliptical shape without abrupt elongation along the y axis indicated an absence of intra-cycle strain-stiffing happened within a period of oscillatory shear (Ewoldt, Hosoi, & McKinley, 2008; Grand & Petekidis, 2008; Lee & Wagner, 2003). Such a result suggests that the material response time for strain thickening is longer than the time scale of the oscillation.

The rheological behavior of gelatinized WMS pastes presented in this paper is different from that of the concentrated hard sphere thickening systems reported earlier (Lee & Wagner, 2003). These authors reported that the hard sphere system (colloidal silica with a particle concentration of about 40%, w/w) with strain thickening behavior could display distinctly different Lissajous curves between nonlinear region of strain thinning and strain thickening. Furthermore, in their study the Lissajous curves within the strain-thickening range displayed both intra-cycle strain thickening (at the maximum strain of the cycle) and intra-cycle strain thinning within the same period (Lee & Wagner, 2003). These differences can be ascribed to different microscopic morphologies and

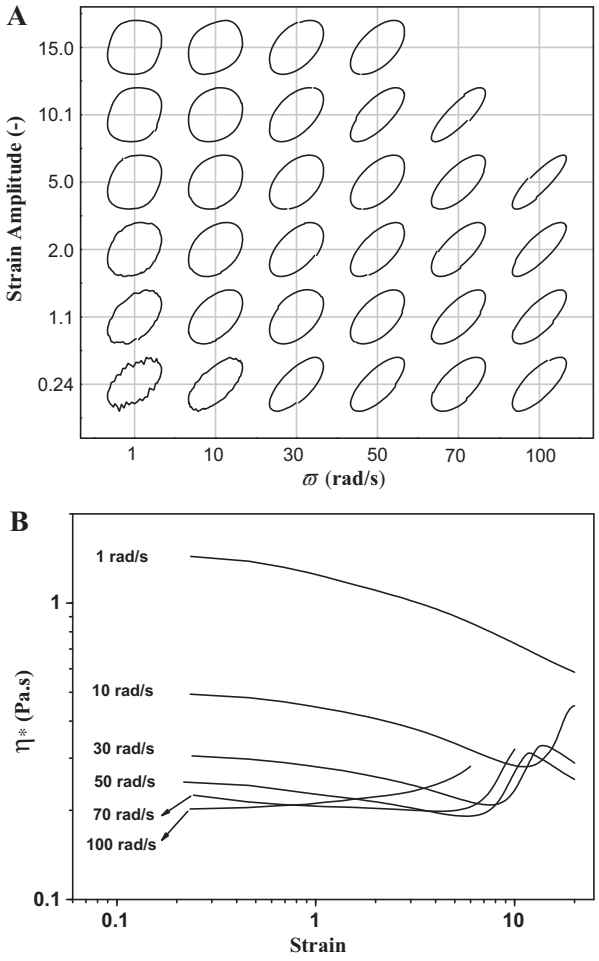

Fig. 5. The normalized Lissajous curves ($\tau(t)/\tau_o$ versus $\gamma(t)/\gamma_o$) of 6.0% (w/w) waxy maize starch pastes for different angular frequencies and strains as indicated (A) and corresponding rheological curves from strain sweeps (B).
Fig. 5(B) is adapted from Wang et al. (2011).

shear-thickening mechanisms between the two systems. For the concentrated hard-sphere systems, the intra-cycle strain-stiffing can be ascribed to collision between the spheres caused by increasing strain. This resulted into the distortion of Lissajous plot at the end of strain (Grand & Petekidis, 2008).

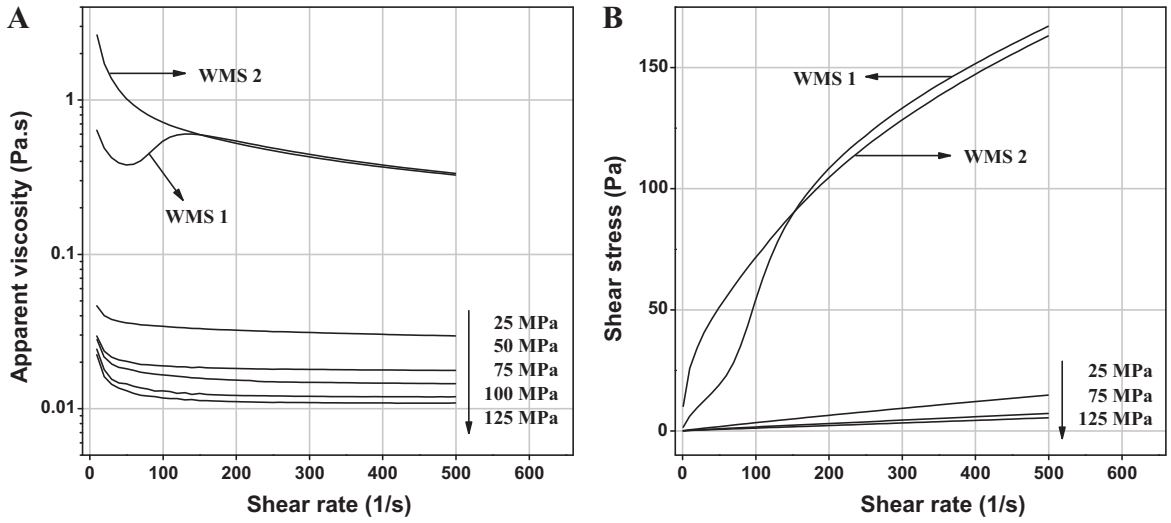

Fig. 6. Continuous steady flow properties of 6.0% (w/w) waxy maize starch pastes subjected to high-pressure homogenization at different homogenizing pressures. All these steady shear tests were conducted in a linear mode.

In this study, the WMS system having low concentration (6.0.%, w/w) was obviously different from the concentrated hard sphere systems. As reported earlier, continuous phase (solution of amylopectin) is responsible for the thickening behavior of WMS systems. This probably is the main reason why the response time for shear thickening in the WMS pastes is longer than the time scale of oscillation. It is easy to comprehend that the conformation change of the amylopectin micro-network should be less sensitive to both strain and the angular frequency than the concentrated solid particles. Due to the slow response of amylopectin network in continuous phase, no strain-thickening was observed in the Lissajous curves of 6% (w/w) WMS pastes. Because of this reason Lissajous curves produced similar shapes both in strain-thickening and strain-thinning stages. However, it has to be noted that the time scale of the oscillatory shear period should be enough to produce strain thickening. This is the reason why the strain thickening could be observed in this study. Because of the slow response of the continuous phase, strain-thickening in this study happened at highly nonlinear range with high frequencies.

3.4. *Effect of high-pressure homogenization on rheological properties of WMS pastes*

The steady shear viscometric data of the WMS samples subjected to high pressure homogenization (HPH) are presented in Fig. 6 (panel A and B). The power law parameters obtained by fitting the power law equation with the experimental shear stress (τ) versus shear rate ($\dot{\gamma}$) data are provided in Table 1. The consistency index (K), flow behavior index (n), and apparent viscosity at shear rate of 200 s^{-1} ($\eta_{a,200}$) are given as a function of homogenizing pressure for both up and down shear ramps. Flow curves (η_a and τ versus $\dot{\gamma}$) are given in Fig. 6(A) and (B). From Table 1 and Fig. 6(A), significant thinning effect is observed in WMS pastes which were subjected to HPH. After HPH treatment at different pressures, all WMS pastes displayed apparent viscosities an order of magnitude lower compared to the un-homogenized ones. The apparent viscosity exhibited a general decreasing trend with increase in the HPH pressure. For example, the apparent viscosity of the WMS paste when subjected to 125 MPa HPH was 0.010/0.010 Pa s (at 200 s^{-1} for up/down ramps), which is about 1/50 of the apparent viscosity of unhomogenized pastes (about 0.5 Pa s at 200 s^{-1} for up/down ramps).

Such a significant decrease in apparent viscosity can be ascribed to fragmentation of starch ghost granules as well as degradation of amylopectin caused by HPH. This is because the HPH is an intensive mechanical process used in producing dispersions and emulsions. During the HPH process, solutions/suspensions experience high pressure, high shear, turbulence, cavitation and temperature increase caused by rapid change in pressure. The shear rate during this process can be as high as 10^5 s^{-1} (Nayouf et al., 2003). Due to the intense mechanical effect, it is reasonable to expect that the rheological behavior of WMS pastes to be significantly affected by the HMS process. The very strong and intense mechanical action of HPH was found to affect the size and size distribution of polysaccharide molecules leading to the molecular fragmentation (decrease in the molecular weight) of HPH on modified starch and xanthan gum (Modig, Nilsson, Bergenstahl, & Wahlund, 2006; Nilsson, Leeman, Wahlund, & Bergenstahl, 2006; Viturawong et al., 2008). Fig. 7 shows the extent of fragmentation of starch ghost particles caused by HPH. Even after the application of HPH at 125 MPa, there still are smaller remnant ghost particles from gelatinized starch granules (Fig. 7(D)). However, after removing these scraps from the homogenized samples by high-speed centrifugation (6000 rpm for 10 min), the apparent viscosity of the sample remained unchanged (data not given). This result indicates the fact that the apparent viscosity of the homogenized samples is controlled by the free or leached amylopectin in the continuous phase. Since that free amylopectins can be degraded to a higher extent at higher homogenizing pressure, thus the apparent viscosity showed a decreasing trend with the increase in homogenizing pressure.

In the absence of HPH treatment, both the 6% (w/w) WMS pastes with/without pre-shearing treatment (WMS 2 and WMS 1, respectively) displayed distinct pseudo-plastic flow behavior with flow behavior index (n) values ranging from 0.49 to 0.67. However, after HPH treatment, the WMS pastes had much lower apparent viscosity and behaved as Newtonian fluid with n values close to unity (the n values ranged from 0.91 to 1.03 in the homogenized samples). The alteration in the flow behavior of WMS pastes due to the use of HPH can be directly observed in Fig. 6(B). In the case of WMS samples without HPH treatment (WMS 1 and WMS 2), the curves (τ versus $\dot{\gamma}$) are nonlinear indicating a non-Newtonian flow behavior. In the case of the homogenized samples, the plot of τ versus $\dot{\gamma}$ is linear, indicating a Newtonian flow behavior. These results are indicative of the degradation/fragmentation effect of HPH on the

Table 1
The power-law parameters and apparent viscosity ($\eta_{a,200}$, Pa s) for the WMS pastes treated under different conditions.[a,b]

Samples	Up curve				Down curve			
	K (Pa s^n)	n	$\eta_{a,200}$ (Pa s)	R^2	K (Pa s^n)	n	$\eta_{a,200}$ (Pa s)	R^2
WMS 1	2.83 ± 0.18^a	0.67 ± 0.01^a	0.54 ± 0.01^a	0.963	7.63 ± 0.07^a	0.49 ± 0.00^a	0.51 ± 0.00^a	0.998
WMS 2	7.40 ± 0.07^b	0.50 ± 0.00^b	0.53 ± 0.00^b	0.999	7.75 ± 0.05^b	0.49 ± 0.00^a	0.50 ± 0.00^b	0.998
25 MPa	0.052 ± 0.001^c	0.91 ± 0.00^c	0.032 ± 0.000^c	1.000	0.045 ± 0.000^c	0.93 ± 0.00^b	0.031 ± 0.000^c	1.000
50 MPa	0.026 ± 0.004^c	0.93 ± 0.02^{cd}	0.019 ± 0.000^d	1.000	0.018 ± 0.000^c	0.99 ± 0.00^c	0.017 ± 0.000^d	1.000
75 MPa	0.020 ± 0.001^c	0.95 ± 0.01^d	0.015 ± 0.000^{de}	1.000	0.014 ± 0.000^c	1.00 ± 0.00^d	0.014 ± 0.000^{de}	1.000
100 MPa	0.015 ± 0.001^c	0.96 ± 0.01^d	0.012 ± 0.000^e	1.000	0.0098 ± 0.0003^c	1.03 ± 0.00^e	0.011 ± 0.000^{ef}	1.000
125 MPa	0.014 ± 0.000^c	0.96 ± 0.00^d	0.011 ± 0.000^e	1.000	0.0091 ± 0.0002^c	1.02 ± 0.00^e	0.010 ± 0.000^f	1.000

[a] Assays were performed in triplicate at 25 °C. Mean ± standard deviation values in the same column for each solution followed by different superscripts are significantly different ($p \leq 0.05$).
[b] "WMS 1" and "WMS 2" both refer to 6% WMS pastes without high-pressure homogenization treatment. The difference is WMS 2 was pre-sheared at 600 s^{-1} for 1 min and equilibrated for 10 s, while WMS 1 without pre-shear.

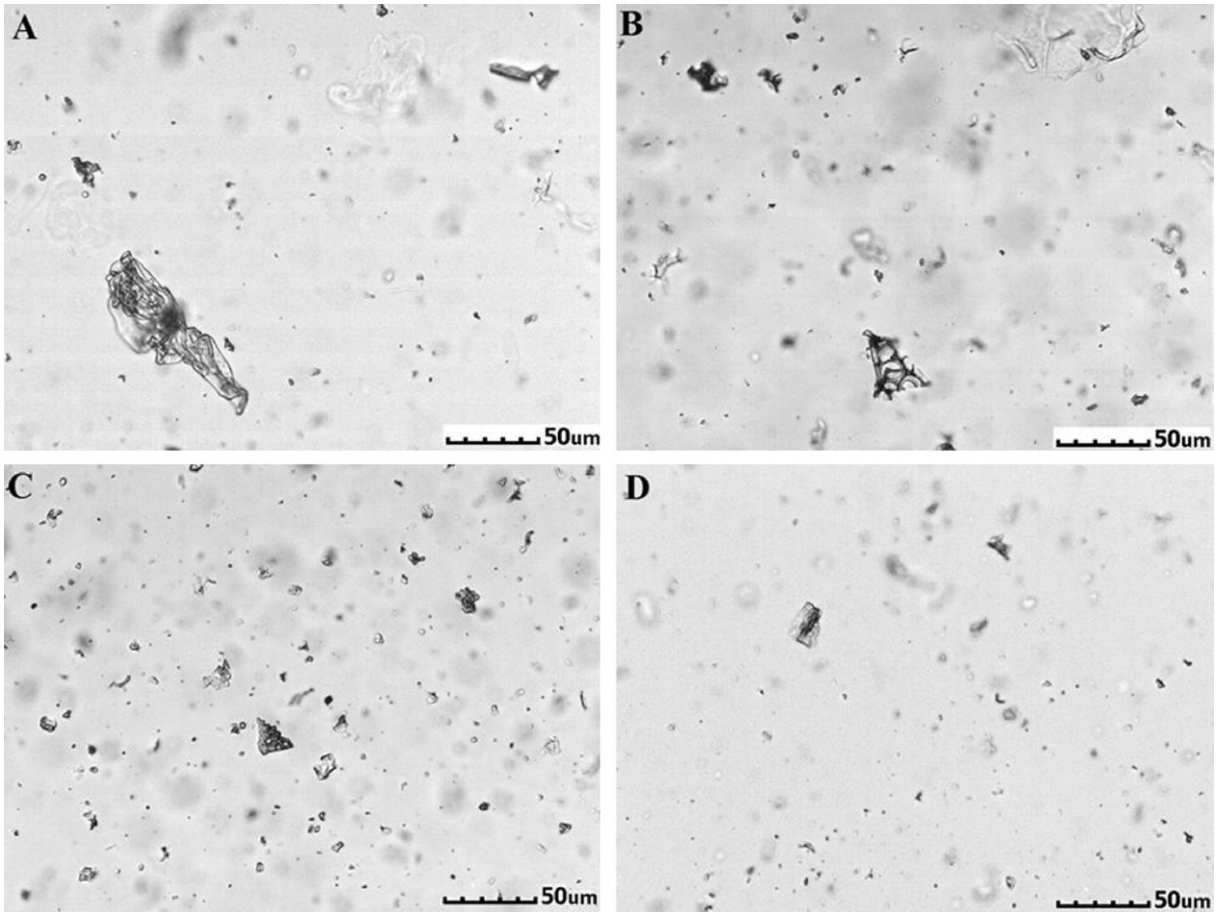

Fig. 7. Microphotographs of the 6.0% (w/w) waxy maize starch pastes: unhomogenized WMS paste (A); WMS pastes homogenized at 25 MPa (B), 75 MPa (C), and 125 MPa (D).

microstructure of the WMS pastes. Due to the fragmentation of the amylopectin, the entanglement between chains of macromolecules can be decreased to a great extent. Because of this reason, the susceptibility of apparent viscosity to shear rate can be significantly decreased in homogenized WMS pastes and makes them behave more like Newtonian fluids.

4. Conclusions

In this study, we investigated the rheological behavior of 6.0% (w/w) hydrothermally gelatinized waxy maize starch pastes. Results from steady shear tests showed that the waxy maize starch pastes displayed shear-thickening in the first up ramp due to the re-arrangement of amylopectin network in the continuous phase at critical shear rate range (about 40–100 s^{-1}). The structural change responsible for shear-thickening was found to be irreversible when the pastes were subjected to pre-shearing at 600 s^{-1} and equilibrated for 6 h at 25 °C. Lissajous curves obtained from large amplitude oscillatory shear tests had similar shapes during nonlinear strain sweep at higher angular frequencies (30–100 rad/s) due to slow response of amylopectin macromolecules in the continuous phase. High pressure homogenization is found to cause significant reduction in the apparent viscosity in the WMS pastes. The apparent viscosity of the homogenized waxy maize pastes decreased as the homogenization pressure increased. The high pressure homogenized waxy maize starch pastes behaved like Newtonian fluids.

Acknowledgements

This research was supported by National Natural Science Foundation of China (30800662, 31000813), Program for New Century Excellent Talents in University of China (NCET-08-0537), Science and Technology Support Project of China (2009BADA0B03), High Technology Research and Development Program of China (2009AA043601), and Commonweal Guild Agricultural Scientific Research Project of China (201003077).

References

Achayuthakan, P., & Suphantharika, M. (2008). Pasting and rheological properties of waxy corn starch as affected by guar gum and xanthan gum. *Carbohydrate Polymers*, *71*, 9–17.

Barnes, H. A., Hutton, J. F., & Walters, K. (1989). *An introduction to rheology*. New York: Elsevier Applied Science., pp. 11–35.

Che, L. M., Wang, L. J., Li, D., Bhandari, B., Özkan, N., Chen, X. D., et al. (2009). Starch pastes thinning during high-pressure homogenization. *Carbohydrate Polymers*, *75*, 32–38.

Debet, M. R., & Gidley, M. J. (2007). Why do gelatinized starch granules not dissolve completely? Roles for amylose, protein, and lipid in granule Ghost integrity. *Journal of Agricultural and Food Chemistry*, *55*, 4752–4760.

Dintzis, F. R., & Bagley, E. B. (1995). Shear-thickening and transient flow effects in starch solutions. *Journal of Applied Polymer Science*, *56*, 637–640.

Dintzis, F. R., Berhow, M. A., Bagley, E. B., Wu, Y. V., & Felker, F. C. (1996). Shear-thickening behavior and shear-induced structure in gently solubilized starches. *Cereal Chemistry*, *73*, 638–643.

Ewoldt, R. H., Hosoi, A. E., & McKinley, G. H. (2008). New measures for characterizing nonlinear viscoelasticity in large amplitude oscillatory shear. *Journal of Rheology*, *52*, 1427–1458.

Gouveia, L. M., Muller, A. J., Marchal, P., & Choplin, L. (2008). Time effects on the rheological behavior of hydrophobically modified polyacrylamide aqueous solutions mixed with sodium dodecyl sulfate (SDS). *Colloids and Surfaces A: Physicochemical and Engineering Aspects*, *330*, 168–175.

Grand, A. L., & Petekidis, G. (2008). Effects of particle softness on the rheology and yielding of colloidal glasses. *Rheologica Acta*, *47*, 579–590.

Hyun, K., Kim, S. H., Ahn, K. H., & Lee, S. J. (2002). Large amplitude oscillatory shear as a way to classify the complex fluids. *Journal of Non-Newtonian Fluid Mechanics*, *107*, 51–65.

Hyun, K., Wilhelmb, M., Klein, C. O., Choc, K. S., Nam, J. G., Ahn, K. H., et al. (2011). A review of nonlinear oscillatory shear tests: Analysis and application of large amplitude oscillatory shear (LAOS). *Progress in Polymer Science*, *36*, 1697–1753.

Indei, T. (2007). Necessary conditions for shear thickening in associating polymer networks. *Journal of Non-Newtonian Fluid Mechanics*, *141*, 18–42.

Kaur, L., Singh, J., Singh, H., & McCarthy, O. J. (2008). Starch–cassia gum interactions: A microstructure – Rheology study. *Food Chemistry*, *111*, 1–10.

Kim, S., Willett, J. L., Carriere, C. J., & Felker, F. C. (2002). Shear-thickening and shear-induced pattern formation in starch solutions. *Carbohydrate Polymers*, *47*, 347–356.

Kulicke, W. M., Eidam, D., Kath, F., Kix, M., & Kull, A. H. (1996). Hydrocolloids and rheology: Regulation of visco-elastic characteristics of waxy rice starch in mixtures with galactomannans. *Starch/Stäerke*, *48*, 105–114.

Leblanc, J. L. (2007). Nonlinear viscoelastic characterization of molten thermoplastic vulcanizates (TPV) through large amplitude harmonic experiments. *Rheologica Acta*, *46*, 1013–1027.

Lee, Y. S., & Wagner, N. J. (2003). Dynamic properties of shear thickening colloidal suspensions. *Rheologica Acta*, *42*, 199–208.

Lehmann, A., Volkert, B., Fischer, S., Schrader, A., & Nerenz, H. (2008). Starch based thickening agents for personal care and surfactant systems. *Colloids and Surfaces A: Physicochemical and Engineering Aspects*, *331*, 150–154.

Loh, J. (1992). The effect of shear rate and strain on the pasting behavior of food starches. *Journal of Food Engineering*, *16*, 75–89.

Mendez-Montealvo, G., Wang, Y. J., & Campbell, M. (2011). Thermal and rheological properties of granular waxy mutant starches after β-amylase modification. *Carbohydrate Polymers*, *83*, 1106–1111.

Modig, G., Nilsson, L., Bergenstahl, B., & Wahlund, K. G. (2006). Homogenization-induced degradation of hydrophobically modified starch determined by asymmetrical flow field-flow fractionation and multi-angle light scattering. *Food Hydrocolloids*, *20*, 1087–1095.

Nayouf, M., Loisel, C., & Doublier, J. L. (2003). Effect of thermomechanical treatment on the rheological properties of crosslinked waxy corn starch. *Journal of Food Engineering*, *59*, 209–219.

Nilsson, L., Leeman, M., Wahlund, K.-G., & Bergenstahl, B. (2006). Mechanical degradation and changes in conformation of hydrophobically modified starch. *Biomacromolecules*, *7*, 2671–2679.

Preiss, J. (1991). Biology and molecular biology of starch synthesis and its regulation. *Oxford Surveys of Plant Molecular and Cell Biology*, *7*, 59–114.

Rodríguez-Hernández, A. I., Durand, S., Garnier, C., Tecante, A., & Doublier, J. L. (2006). Rheology-structure properties of waxy maize starch–gellan mixtures. *Food Hydrocolloids*, *20*, 1223–1230.

Sands, A. L., Leidy, H. J., Hamaker, B. R., Maguire, P., & Campbell, W. W. (2009). Consumption of the slow-digesting waxy maize starch leads to blunted plasma glucose and insulin response but does not influence energy expenditure or appetite in humans. *Nutrition Research*, *29*, 383–390.

Steffe, J. F. (1996). *Rheological methods in food process engineering* (2rd ed.). East Lansing: Freeman., pp. 22–28.

Viturawong, Y., Achayuthakan, P., & Suphantharika, M. (2008). Gelatinization and rheological properties of rice starch/xanthan mixtures: Effects of molecular weight of xanthan and different salts. *Food Chemistry*, *111*, 106–114.

Wang, B., Li, D., Wang, L. J., & Özkan, N. (2010). Anti-thixotropic properties of waxy maize starch dispersions with different pasting conditions. *Carbohydrate Polymers*, *79*, 1130–1139.

Wang, B., Wang, L. J., Dong Li Zhou, Y. G., & Özkan, N. (2011). Shear-thickening properties of waxy maize starch dispersions. *Journal of Food Engineering*, *107*, 415–423.